Eur. Phys. J. B **15**, 247–251 (2000)

THE EUROPEAN PHYSICAL JOURNAL B

EDP Sciences

Specific-heat study of the triangular-lattice antiferromagnet $RbCuCl_3$

F. Pérez-Willard[1,a], A. Faißt[1], J. Wosnitza[1], H. v. Löhneysen[1], U. Schotte[2], and H. Tanaka[3]

[1] Physikalisches Institut, Universität Karlsruhe, Engesserstrasse 7, 76128 Karlsruhe, Germany
[2] Hahn-Meitner-Institut, 14109 Berlin, Germany
[3] Department of Physics, Faculty of Science, Tokyo Institute of Technology, Tokyo 152, Japan

Received 18 October 1999

Abstract. We report on the magnetic phase diagram of the distorted triangular-lattice antiferromagnet $RbCuCl_3$ for a magnetic field applied parallel to the basal plane ($B \perp c$). High-resolution measurements of the specific heat and of the magnetocaloric effect have been performed in magnetic fields up to 14 T. The high-field specific-heat data reveal the existence of an intermediate phase between the paramagnetic and the frustrated antiferromagnetic phase.

PACS. 75.40.Cx Static properties (order parameter, static susceptibility, heat capacities, critical exponents, etc.) – 75.50.Ee Antiferromagnetics – 64.60.Fr Equilibrium properties near critical points, critical exponents

1 Introduction

ABX_3 compounds, where A^+ stands for an alkaline-metal ion, B^{2+} for a transition-metal ion, and X^- for a halogenide ion have been studied extensively in recent years [1]. These materials usually crystallize in a hexagonal $P6_3/mmc$ structure, where the magnetic B^{2+} ions form two-dimensional triangular sublattices which are stacked along the crystallographic c direction. ABX_3 systems behave as quasi-one-dimensional magnets because of the strong nearest-neighbor coupling J_c perpendicular to the triangular sublattices. The much weaker antiferromagnetic superexchange coupling J_{ab} between nearest B^{2+} neighbors in the triangular planes causes frustration of the in-plane neighboring magnetic moments below the three-dimensional (3D) ordering temperature T_N of typically 10 K. The magnetic moments order in a 120° spin structure with a two-fold degeneracy of the ground state.

The spin system of an ideal triangular-lattice antiferromagnet can be described by the Hamiltonian

$$H = -J_c \sum_{i,j} \mathbf{S}_i \mathbf{S}_j - J_{ab} \sum_{i,j} \mathbf{S}_i \mathbf{S}_j + D \sum_i (S_i^z)^2 - g\mu_B \mathbf{B} \sum_i \mathbf{S}_i. \quad (1)$$

The first two sums describe the spin coupling between nearest neighbors along the c-direction and in the triangular basal plane, respectively. D is the anisotropy constant, where $D > 0$ corresponds to an easy-plane anisotropy (XY system), while $D < 0$ describes an easy-axis anisotropy. The last term takes into account the Zeeman energy of the spins in an external field $\mathbf{B}$.

Some intensively studied examples of ideal stacked triangular-lattice antiferromagnets are $CsMnBr_3$ (XY system), $CsNiCl_3$, and $CsMnI_3$ (both easy-axis systems) [2]. They all keep the crystallographic $P6_3/mmc$ structure down to lowest temperatures. Common to these systems are their rich magnetic (B, T) phase diagrams and a critical behavior that strongly deviates from the universality classes of unfrustrated systems [1].

The Hamiltonian (1) must be extended with additional terms when dealing with "non-ideal" ABX_3 systems that undergo structural phase transitions from the ideal hexagonal high-temperature $P6_3/mmc$ phase to less symmetric phases with decreasing temperature. The loss in structural symmetry leads to modified magnetic interactions between the B^{2+}-ion spins resulting in a partial release of magnetic frustration.

One example for a "non-ideal" triangular-lattice antiferromagnet is $CsCuCl_3$ which undergoes a first-order structural phase-transition at 423 K into a $P6_122$ structure [3]. This transition is due to the cooperative Jahn-Teller effect, which is extraordinarily large for Cu^{2+}-ions in an octahedral environment of anions [4]. The lack of inversion symmetry in the low-temperature structure introduces an additional Dzyaloshinskii-Moriya (DM) term

$$H_{DM} = \sum_{i,j} \mathbf{D}_{ij} \cdot (\mathbf{S}_i \times \mathbf{S}_j) \quad (2)$$

in the Hamiltonian (1). The DM interaction and the dominating ferromagnetic interaction along the c axis result

[a] e-mail: fabian.perez@phys.uni-karlsruhe.de

in an incommensurate winding of the Cu^{2+} $S = 1/2$ spins with a pitch angle of about 5° [5]. Furthermore, the DM interaction acts as an easy-plane anisotropy forcing the Cu^{2+} spins to lie almost flat in the ab plane. Hence, within a good approximation the spin system of $CsCuCl_3$ is an XY system although the anisotropy constant is very small. Therefore in zero magnetic field one would expect the critical behavior of a 3D chiral XY system whereas our specific-heat results [6] show a crossover to a weak first-order transition below a reduced temperature $t = |(T_N - T)/T_N| \approx 10^{-3}$ in agreement with recent numerical simulations [7].

The small value $S = 1/2$ of Cu^{2+} spins enhances the role of quantum fluctuations which lead to (B, T) phase diagrams of $CsCuCl_3$ with multiple phases for both $B \parallel c$ and $B \perp c$ [8]. We have studied the phase diagrams of $CsCuCl_3$ for $B \parallel c$, $B \perp c$, and oblique field orientation by means of specific heat, magnetization and neutron scattering experiments [6,9].

The closely related compound $RbCuCl_3$ is less extensively investigated, with focus on the structural phase transitions which — as in $CsCuCl_3$ — are the result of a cooperative Jahn-Teller effect. At $T_1 = 339$ K, $RbCuCl_3$ transforms from the hexagonal high-temperature structure to an orthorhombic structure (space group Pbcn) doubling its unit cell along the b direction. A further transition at $T_2 = 260$ K doubles the lattice parameter along the c axis reducing the symmetry to a monoclinic structure (space group C2) [10]. Both structural phase transitions seem to be of first order [11].

Tazuke *et al.* [12] observed an antiferromagnetic phase transition in the magnetic susceptibility of $RbCuCl_3$ at 19 K and estimated the values of J_c and J_{ab} to be of the same magnitude as those of $CsCuCl_3$, but of opposite sign, *i.e.* antiferromagnetic coupling along the c direction and ferromagnetic coupling in the ab plane, therefore, excluding the possibility of a frustrated triangular antiferromagnet. On the other hand, very recent neutron-diffraction measurements [13] show Bragg peaks below $T_N \approx 19$ K which correspond to a chiral arrangement of the spins in the basal plane. The measured vector $\mathbf{Q} = (0.2993, 0.2993, 0)$ is incommensurate to the underlying lattice leading only to partial frustration. It differs from the wave vector $\mathbf{Q} = (1/3, 1/3, 0)$ of an ideal triangular arrangement of the spins (found for example in $CsMnBr_3$) in that the in-plane turn angle is about 108° instead of 120°. The exchange constants are estimated in this experiment to $J_c = 25$ K (ferromagnetic coupling) and $J_{ab} = -9.6$ K (antiferromagnetic coupling) contrary to the estimates of Tazuke *et al.*

Another partially frustrated compound showing an incommensurate spiraling of the spins in the ab plane is $RbMnBr_3$ [14]. Here, the turn angle is about 130°. For a theoretical description of the spin structure two different magnetic interactions J_{ab1} and J_{ab2} in the basal plane have been introduced [15] because the orthorhombic crystal distortion in the low-temperature phase of $RbMnBr_3$ leads to nonequivalent bond lengths within the ab plane. Based on the structural distortions in $RbCuCl_3$ a similar assumption seems to be highly plausible in order to explain the incommensurate magnetic structure.

The present investigation was aimed at studying the magnetic phase diagram of $RbCuCl_3$ for the magnetic field direction $B \perp c$ in order to compare qualitatively its topology with the well-known phase diagrams of $CsCuCl_3$ and $RbMnBr_3$. $RbCuCl_3$ shares with $CsCuCl_3$ the same B^{2+} and X^- ions, and with $RbMnBr_3$ the incommensurate spin structure at low temperatures [13,14]. To our knowledge, no specific-heat data have been reported on $RbCuCl_3$ before.

2 Experiment

The $RbCuCl_3$ sample was cleaved from a single crystal grown by the Bridgman technique. The specific heat C of the sample was measured between 4.2 K and 30 K by a standard semiadiabatic heat-pulse technique in applied magnetic fields up to 14 T. The same experimental setup was also used to measure the magnetocaloric effect $\left(\frac{\delta T}{\delta B}\right)_S = -\frac{T}{C}\left(\frac{\delta S}{\delta B}\right)_T$ of the sample.

The temperature resolution $\delta T/T$ of our experiment is given by the temperature sensitivity of the Allen-Bradley resistor used as sample thermometer. At 20 K, $\delta T/T < 1 \times 10^{-5}$ allows small heat pulses with temperature increments $\Delta T/T < 1 \times 10^{-3}$ at the transitions. The absolute value of the measured temperatures have error bars of ±2% due to calibration errors of the thermometer. Further experimental details can be found in reference [16].

3 Results and discussion

The specific heat of $RbCuCl_3$ between 4.2 K and 30 K at zero magnetic field and at the highest field of 14 T is shown in Figure 1 in a double-logarithmic plot. The magnetic field was applied parallel to the sample's basal plane ($B \perp c$). Both curves overlap over almost the whole temperature range. At low temperatures the specific heat is approximately proportional to T^3, composed of a phononic Debye T^3 contribution and a magnetic T^3 contribution from antiferromagnetic magnons.

Both specific-heat curves in Figure 1 reveal anomalies in a small temperature window around 18.5 K (see inset of Fig. 1). At first glance (we will come back to this point later) only one sharp anomaly is seen for $B = 0$ at a critical temperature $T_c = (18.88 \pm 0.01)$ K which is in good agreement with the value deduced from susceptibility measurements of Tazuke *et al.* [12]. Below T_c, the Cu^{2+} spins order antiferromagnetically in the ab plane and form the mentioned incommensurate chiral spin structure with a turn angle [13] of about 108° (C phase). At $B = 14$ T two anomalies at $T_{c1} = (18.31 \pm 0.02)$ K and $T_{c2} = (18.69 \pm 0.09)$ K can be clearly resolved indicating an intermediate magnetic phase (I phase).

A compilation of our specific-heat data on $RbCuCl_3$ for several magnetic fields B in the interesting temperature range around 18.5 K is presented in Figure 2. The temperature range where the intermediate phase exists becomes

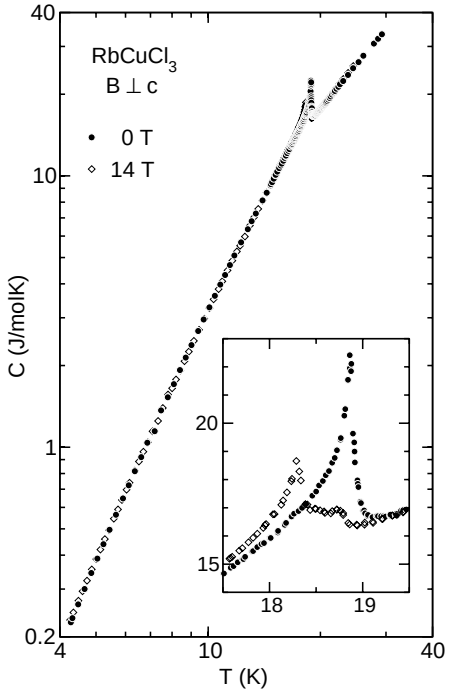

Fig. 1. Specific heat C *vs.* temperature T of $RbCuCl_3$ for $B = 0$ and $B = 14$ T ($B \perp c$) in a double-logarithmic plot. The inset shows the data between 17 and 20 K in a linear plot. At $B = 14$ T two anomalies are clearly resolved.

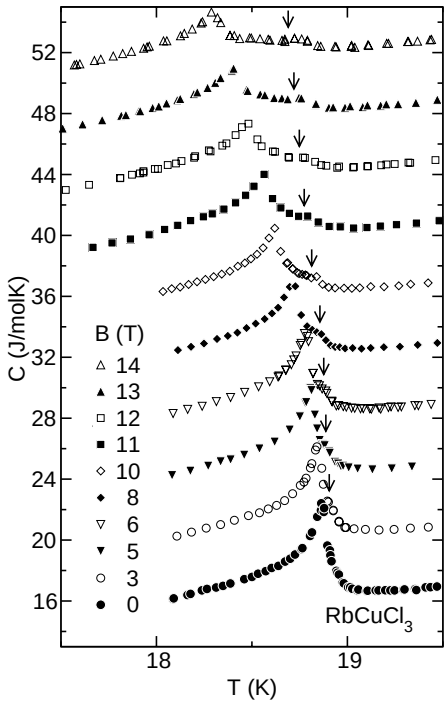

Fig. 2. Specific heat C *vs.* temperature T of $RbCuCl_3$ for selected magnetic fields perpendicular to the sample's c axis. For clarity, the values of C are shifted upward consecutively by 4 J/molK with increasing field. The arrows denote the estimated transition temperatures T_{c2}.

narrower with decreasing magnetic field. For $B = 3$ T the anomaly at T_{c2} can hardly be resolved and appears only as a weak shoulder on the high-temperature side of the main T_{c1} peak. The evolution of C in magnetic field suggests that the more pronounced peaks measured at T_{c1} for $B \neq 0$ belong to the same phase boundary as the zero-field anomaly (see also Fig. 4). The height of the T_{c1} anomaly weakens with increasing field while that at T_{c2} remains roughly constant.

Figure 3 shows the magnetocaloric effect $\Delta T/\Delta B$ of $RbCuCl_3$ measured at 5.0 K and 18.6 K. Because of the small size of the effect large magnetic field steps of 200 mT were utilized in order to keep the scatter of the data acceptable. The 5.0-K curve shows a smooth field dependence of $\Delta T/\Delta B$ with a broad maximum around 2.5 T and no indication for an anomaly. A second field run at 18.55 K attempted to cross the boundary between the phases C and I already determined by means of the specific-heat experiment. Indeed, a step-like anomaly can be seen at $B_c = (11.6 \pm 0.5)$ T consistent with the specific-heat data.

The (B, T) phase diagram of $RbCuCl_3$ for $B \perp c$ extracted from our specific-heat data (filled circles) and magnetocaloric-effect data is shown in Figure 4. The dashed lines drawn as guides to the eye show the phase boundaries. From neutron-diffraction experiments [13] it is known that below T_{c1} an incommensurate chiral spin configuration is stabilized. Above T_{c2}, only short-range one-dimensional ordered magnetic chains but no three-dimensional order is present (PM phase). Between these

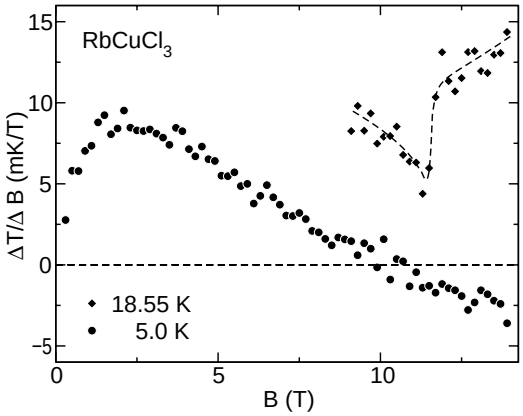

Fig. 3. Magnetocaloric effect $\Delta T/\Delta B$ *vs.* magnetic field B of $RbMnBr_3$ for $T = 5.0$ K and $T = 18.55$ K ($B \perp c$). The $T = 18.55$ K data have an offset of 10 mK/T. The dashed line through the data points at 18.55 K is a guide to the eye.

two phases a third magnetically ordered intermediate one evolves. Further work, in particular high-field neutron-scattering experiments, is planned to elucidate the magnetic structure of this new phase of $RbCuCl_3$.

$RbCuCl_3$ and $RbMnBr_3$ share a similar spin structure with an incommensurate spiraling of the spins within the ab plane [13,14]. For $RbMnBr_3$ a total of five different phases were found [16] in the phase diagram ($B \perp c$), two

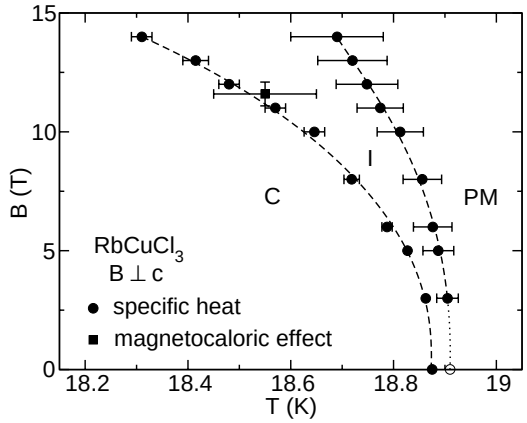

Fig. 4. Magnetic phase diagram of $RbCuCl_3$ for $B \perp c$ as found from specific-heat (circles) and magnetocaloric-effect (square) data. The dashed lines are guides to the eye. The open circle at $B = 0$ is motivated by a weak anomaly seen in Figure 5 (see text).

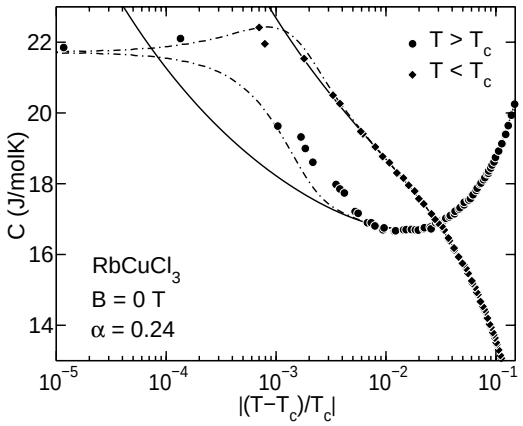

Fig. 5. Specific heat C of $RbCuCl_3$ *vs.* $\log|(T-T_c)/T_c|$ for $B = 0$. The solid lines are fits according to equation (3), the dashed-dotted lines are fits including a Gauss-distributed smearing of T_c with $\delta T_c/T_c = 7.4 \times 10^{-4}$.

chiral phases C_1 and C_2, two spinflop-like phases SF_1 and SF_2, and a short-range one-dimensional phase PM up to 7 T. The two chiral phases as well as the two spinflop-like phases order with slightly different incommensurate ordering vectors [17]. In the present case, for $RbCuCl_3$ we have only detected three phases up to 14 T. This difference might be caused by the small $S = 1/2$ spin of the Cu^{2+} ions in $RbCuCl_3$, which due to quantum fluctuations may prohibit the different incommensurate ordering vectors in the chiral and spin-flop phase.

The behavior of the PM-I phase boundary at low fields ($B \leq 3$ T) remains unclear. An open question is whether the intermediate phase is already present at $B = 0$ or not. In the following we will try to justify why we think that the first possibility is the correct one. Figure 5 shows the C data for $B = 0$ in a semilogarithmic plot *vs.* the reduced temperature $t = (T - T_c)/T_c$ with $T_c = T_{c1} = 18.88 \pm 0.01$ K. We apply the usual fit function

$$C^{\pm} = \frac{A^{\pm}}{\alpha}|t|^{-\alpha} + B + Et \ , \qquad (3)$$

where the superscript + (–) refers to $t > 0$ ($t < 0$). The regular contribution to C is approximated by the linear dependence $(B + E\,t)$ close to T_c and the power law represents the leading contribution to the singularity in C. When a good fit is achieved except very close to T_c, a Gaussian distribution of T_c with width δT_c is introduced, simulating the rounding of the transition. For further details on the fitting procedure see reference [2]. The best fit is achieved for $T_c = 18.88$ K, $\alpha = 0.24 \pm 0.05$ and $\delta T_c/T_c = 7.4 \times 10^{-4}$. Although the data points for $T < T_c$ are well described by this fit, there are strong deviations from the fit for $T > T_c$ in the region $10^{-3} < t \leq 5 \times 10^{-3}$. In fact, no fit parameters could be found to describe simultaneously the data for $T < T_c$ and $T > T_c$ including this region. This observation may be explained by assuming a second transition at $T_{c2} \approx T_c \times (1 + 1.5 \times 10^{-3}) = 18.91$ K which would account for an additional contribution to C not taken into account in equation (3). The open circle in Figure 4 shows the position where T_{c2} at $B = 0$ might be located. This would be in line with the behavior found for $RbMnBr_3$ where the intermediate spin-flop line was also present for $B = 0$. We finally note that the exponent $\alpha = 0.24 \pm 0.05$ and the amplitude ratio $A^+/A^- = 0.48 \pm 0.1$ which correspond to those predicted for a Heisenberg chiral system [1] are probably the result of an averaging over the two neighboring transitions at $B = 0$.

4 Summary

We have presented the magnetic phase diagram up to 14 T of $RbCuCl_3$ for a magnetic field applied parallel to the basal plane ($B \perp c$) as obtained from high-resolution specific-heat and magnetocaloric-effect measurements. A new intermediate phase has been detected at high magnetic fields which may be stabilized in a finite temperature region even at $B = 0$.

References

1. For a review on triangular-lattice antiferromagnets see: M.F. Collins, O.A. Petrenko, Can. J. Phys. **75**, 605 (1997).
2. H.v. Löhneysen, D. Beckmann, J. Wosnitza, D. Visser, J. Magn. Magn. Mater. **140-144**, 1469 (1995); H. Weber, D. Beckmann, J. Wosnitza, H.v. Löhneysen, Int. J. Mod. Phys. B **9**, 1387 (1995).
3. C.J. Kroese, J.C.M. Tindemans van Eyndhoven, W.J.A. Maaskant, Solid. State Commun. **9**, 1707 (1971).
4. J.D. Dunitz, L.E. Orgel, J. Phys. Chem. Solids **3**, 20 (1957).
5. K. Adachi, N. Achiwa, M. Mekata, J. Phys. C **49**, 545 (1980).
6. H.B. Weber, T. Werner, J. Wosnitza, H.v. Löhneysen, U. Schotte, Phys. Rev. B **54**, 15924 (1996).
7. M.L. Plumer, A. Mailhot, J. Phys. C **9**, L165 (1997); D. Loison, K.D. Schotte, Eur. Phys. J. B **5**, 735 (1998).

8. T. Nikuni, H. Shiba, J. Phys. Soc. Jpn **62**, 3268 (1993); A.E. Jacobs, T. Nikuni, J. Phys. Cond. Matter **10**, 6405 (1998).
9. T. Werner, H.B. Weber, J. Wosnitza, A. Kelnberger, M. Meschke, U. Schotte, N. Stüßer, Y. Ding, M. Winkelmann, Solid. State Commun. **102**, 609 (1997); J. Wosnitza, F. Pérez, H.B. Weber, T. Werner, H.v. Löhneysen, U. Schotte, J. Magn. Magn. Mater. **177-181**, 177 (1998).
10. M. Harada, J. Phys. Soc. Jpn **51**, 2053 (1982); M. Harada, J. Phys. Soc. Jpn **52**, 1646 (1983); M. Harada, J. E. Fischer, G. Shirane, Y. Yamada, J. Phys. Soc. Jpn **56**, 3786 (1987).
11. H. Tanaka, H. Dachs, K. Iio, K. Nagata, J. Phys. C **19**, 4861 (1986).
12. Y. Tazuke, S. Kinouchi, H. Tanaka, K. Iio, K. Nagata, J. Phys. Soc. Jpn **55**, 4020 (1986).
13. M. Reehuis, U. Schotte, M. Meschke, to be published.
14. C.J. Glinka, V.J. Minkiewicz, D.E. Cox, C.P. Khattak, AIP Conf. Proc. **18**, 659 (1973).
15. H. Kawamura, Prog. Theor. Phys. Suppl. **101**, 545 (1990); W. Zhang, W. M. Saslow, M. Gabay, Phys. Rev. B **48**, 10204 (1993).
16. F. Pérez, T. Werner, J. Wosnitza, H.v. Löhneysen, H. Tanaka, Phys. Rev. B **58**, 9316 (1998).
17. M.E. Zhitomirsky, Phys. Rev. B **54**, 353 (1996).